A Novel Large-Scale, Multilayer, and Facilely Aligned Micropatterning Technique Based on Flexible and Reusable SU-8 Shadow Masks

Somayeh Moradi,* Nooshin Bandari, Vineeth Kumar Bandari, Feng Zhu,* and Oliver G. Schmidt

A simple method to fabricate flexible, mechanically robust, and reusable SU-8 shadow masks is demonstrated. This shadow mask technology has high pattern flexibility as various shapes with different dimensions can be created. The fabricated shadow masks are characterized in terms of the resolution, reusability, and capability of multilayer surface micropatterning. Fabrication of a new plastic photomask for the exposure process simplifies the shadow mask fabrication process and results in higher resolution in the shadow mask structures compared to the commercial chromium photomasks. For the multilayer surface micropatterning technology, a simple and fast alignment technique based on SU-8 pillars and without usage of any microscopic tools is reported. This unique method leads to a less complicated alignment process with the alignment accuracy of ≈2 μm. The proposed shadow mask technology can be easily employed for wafer-scale micropatterning process. The capability of fabricated SU-8 shadow masks in micropatterning on polymer thin films is evaluated by fabricating metallic contacts on poly(3,4-ethylenedioxythiophene) samples and electrical characterization.

Novel patterning technologies that can enable structuring on complex surfaces are demanded in the next generation of micro- and nano-electromechanical systems. Classical micro- and nanofabrication which is based on optical lithography has

S. Moradi, N. Bandari, V. K. Bandari, Dr. F. Zhu, Prof. O. G. Schmidt
Material Systems for Nanoelectronics
Chemnitz University of Technology
Reichenhainer Straße 70, 09107 Chemnitz, Germany
E-mail: s.moradi@ifw-dresden.de; f.zhu@ifw-dresden.de
S. Moradi, N. Bandari, V. K. Bandari, Dr. F. Zhu, Prof. O. G. Schmidt
Center for Materials
Architectures and Integration of Nanomembranes (MAIN)
Chemnitz University of Technology
Rosenberg Str. 6, 09126 Chemnitz, Germany
S. Moradi, N. Bandari, V. K. Bandari, Dr. F. Zhu, Prof. O. G. Schmidt
Institute for Integrative Nanosciences
Leibniz IFW Dresden
Helmholtzstraße 20, 01069 Dresden, Germany

The ORCID identification number(s) for the author(s) of this article can be found under https://doi.org/10.1002/admt.201900519.

limitations for the patterning of organic materials due to solvent incompatibility, patterning of nontraditional materials like proteins and cells, patterning on plastic substrates that cannot withstand high temperatures, and finally patterning on nonplanar substrates and surfaces containing fragile structures because of the risk of mechanical damage. Developing a versatile and cost-efficient micro- and nanofabrication will be a key factor for further miniaturization of the new applications based on the unconventional structuring processes.[1,2] In recent years, new technologies for micro- and nanostructuring have been developed in different fields in science and engineering.[3] Among these novel patterning technologies, stencil lithography provides unique advantages such as fast and simple processing, large compatibility with various materials, and high adaptability on topography.[4]

Unlike photolithography, which typically involves cyclic processing steps such as material deposition, photoresist coating, thermal treatment, exposure, development, pattern transfer by etching, and finally resist removing, stencil lithography is a simple structuring technology based on shadow mask technique, which allows parallel, resistless micro- and nanopatterning of material through apertures in a membrane onto a substrate. Stencil lithography has become a reliable micro- and nanopatterning technique and has shown great potential especially in many unconventional applications. While the main advantage of the stencil lithography is its compatibility with variety of materials which can be deposited, it can also offer unique capabilities in patterning on flexible substrates[5,6] as well as patterning on top of complex 3D structures.[7,8] Moreover, its resistless nature provides biocompatible environment for many bioapplications.[9–12]

The potential of shadow masks for a broad range of materials, processes, and applications has been demonstrated by numerous reports in the last decades. The shadow masks for micro- and nanopatterning are usually made of thin metals, metallic alloys, and ceramic foils such as Si, SiN, Ni, permalloy, AlOx, and stainless steel with openings fabricated using micromachining, chemical etching, or laser ablation.[13–26] However, these shadow masks are normally rigid and brittle, requiring complicated and expensive processing steps. For example, efficient laser processing of metals and ceramics as a widely used microfabrication technique

needs high laser intensities, where, material properties are approaching their critical limits and ablation mechanisms are becoming complicated. Moreover, despite the extensive studies of laser ablation of a variety of materials, there are still significant inaccuracies in machining a feature of a desired dimensions. Using thin and brittle membranes under harsh conditions is difficult and the growth of thicker layers is also challenging due to stress generated in the layers.

Recently, fabrication of flexible shadow masks based on polymers for micropatterning has attracted a lot of attention. These studies have revealed that the polymeric shadow masks have some advantages over the conventional metal masks, which include the easier fabrication process, higher structure resolution, higher mechanical flexibility, and simpler mask-positioning steps.

In order to select a proper polymeric material to fabricate a flexible shadow mask, several crucial parameters including physical and chemical properties of the polymer, processing conditions, and performance demands of the application need to be considered.

Fabrication of shadow masks using elastomeric polymers such as polydimethylsiloxane (PDMS) has been reported by several groups.[27,28] However, elastomeric shadow masks are mechanically fragile and not easy to handle. Moreover, they have difficulties in achieving mechanical alignment and high-resolution structuring. Parylene-C has been also shown to be amenable for fabricating shadow masks, but its fabrication process is complex and requires multiple time-consuming steps including chemical vapor deposition, thermal evaporation, and reactive ion etching.[29] Flexible membranes made of other polymeric materials such as polyimide (PI), polytetrafluoroethylene, poly(methyl methacrylate) mostly fabricated by laser micromachining have been investigated by many groups.[30–33] However, severe polymer warping during laser cutting, low control over the feature size, and high cost of the process are critical issues. 3D printing of acrylonitrile butadiene styrene shadow masks[34,35] has been also tried, but low resolution, poor edge quality of the printed shadow mask structures, difficulty in fabricating high aspect ratio structures due to the additive nature of the process, and low yield of the printed shadow masks make it still challenging to use this shadow mask technology in microfabrication processes.

Different groups have also reported photoresists as flexible shadow masks. The fabrication of freestanding films made of a 1002F photoresist film[36] or a trilayer of metal, photoresist, and antireflective coating[37,38] have been explored for various stenciling applications. However, the proposed release techniques are based on a time-consuming sacrificial layer removal and may damage the mask membrane.

Popular SU-8 photoresist as a physically and chemically stable and easy-to-process material, which can be an excellent candidate to engineer a flexible shadow mask, has been introduced by several groups.[39–42] Although SU-8 membranes with various thicknesses, dimensions, and structure resolutions for various applications have been demonstrated, none of these reports have characterized the fabricated shadow masks in terms of reusability, robustness, and quality of the shadow mask structures. In fact, high residual stress of SU-8 polymer during processing, which can result in buckling, makes it challenging

to employ SU-8 masks in versatile micropatterning. Especially, wafer-scale micropatterning process by SU-8 shadow masks has not been demonstrated to date.

Here, by applying a new series of SU-8 photoresist to minimize the residual stresses during the fabrication process and exploiting a simple releasing technique, we realize fabrication of a robust, flexible, and reusable shadow mask based on SU-8 polymer. In this novel shadow mask methodology, a large number of mask configurations with different shapes and dimensions can be straightforwardly fabricated. Owing to the less developed residual stress in the SU-8 masks during the processes and a smooth releasing step which enable us to fabricate wafer-scale shadow masks, we effectively prove the large-scale micropatterning process.

We also develop a fast and simple alignment technique without the need for any microscopic tools to demonstrate the capability of the proposed technique in multilayer micropatterning process. By employing this novel alignment method, we successfully carry out for the first time wafer-scale multilayer micropatterning by SU-8 shadow mask technology. Moreover, as one of the main potential applications of this technology, structuring of the metallic electrodes on surface of the organic thin films has been evaluated in this report.

The sequence of the steps for the fabrication of this novel SU-8 shadow mask is illustrated in **Figure 1**a. After cleaning a Si substrate by means of the organic solvents under the ultrasonic conditions, the process begins by depositing a layer of PDMS on surface of the substrate as an adhesive layer. Afterward, a 50 μm thick PI layer is adhered to the PDMS layer to be used as a releasing layer at the end of the fabrication process.[43] Although, the adhesion of the PI layer to the PDMS surface relies on weak van der Waals forces, but it is enough sufficient to fix PI sheet to the substrate during the whole fabrication steps. Further, a new series of SU-8 photoresist is spin-coated on top of PI layer. The new formulation in these SU-8 series results in improving the adhesion and reducing the residual stress of the coated layers. Due to high viscosity of SU-8 photoresist, which can result in the edge bead effect upon spin-coating process, deposition process of the thick SU-8 layers should be done in two steps including spin-coating and volume-injection processes.[44]

The baking process to evaporate the extra solvents and densify SU-8 layer is done on a typical hot plate in several steps with different baking temperatures and times. A slow cooling step is necessary for the recrystallization process.[41] After preparation of the SU-8 layer, it is exposed through a self-made plastic photomask with the desired patterns, which is gently placed onto the SU-8 layer. The SU-8 patterning process is followed by the postbaking and development processes to transfer the structures to SU-8 layer. Finally, the fabricated SU-8 shadow mask is mechanically peeled off from the substrate by means of a tweezer. The SU-8 surface remains perfectly undamaged after the peeling process due to the poor adhesion between the layers.

Since there is a direct relation between the photolithography parameters and the resolution of the shadow mask microstructures, we investigated the effect of UV exposure dosage and duration of UV radiation as the most relevant parameters in providing the sufficient energy for the SU-8 layers to be fully cross-linked. Considering a fixed light density, any changes in the exposure time can lead to an inevitable loss of resolution. Based
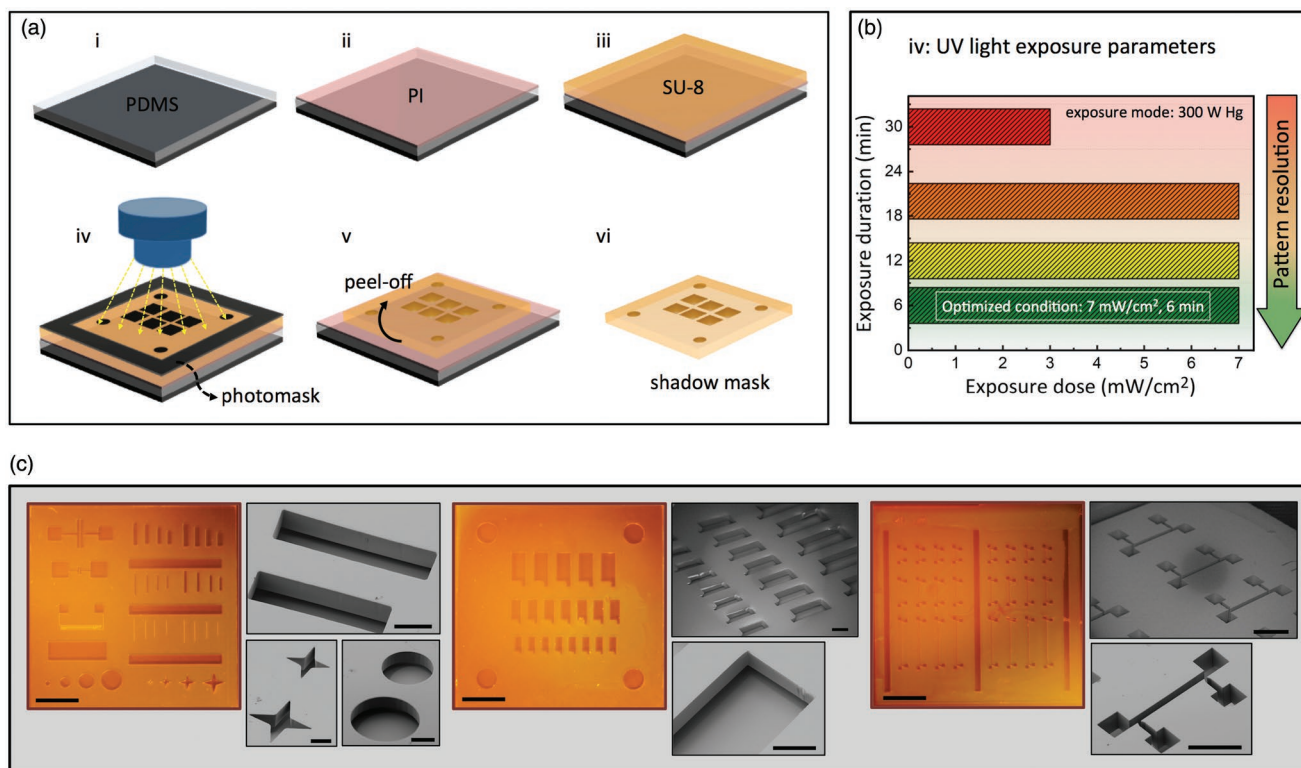
**ADVANCED
SCIENCE NEWS**
www.advancedsciencenews.com

**ADVANCED
MATERIALS
TECHNOLOGIES**
www.advmattechnol.de

Figure 1. Fabrication of SU-8 shadow mask. a) A Schematic illustration showing the fabrication steps of the SU-8 shadow mask. The process begins by depositing a layer of PDMS on the substrate surface as an adhesive layer. Afterward, a 50 µm thick polyimide (PI) layer is adhered to the PDMS layer to be used as a releasing layer at the end of the fabrication process. Further, a new series of SU-8 photoresist is spin-coated on top of PI layer. After preparation of the SU-8 layer, it is exposed through a self-made plastic photomask to transfer the patterns to the SU-8 layer. Finally, the fabricated SU-8 shadow mask is mechanically peeled off from the substrate by means of a tweezer. b) Optimized parameters for the exposure process of the SU-8 shadow mask patterning step. c) Photographs of the fabricated SU-8 shadow mask compromising of the structures with different shapes and dimensions which demonstrate high pattern flexibility of the proposed technology. Scale bars are 2 mm. SEM images reveal the sidewall quality of the shadow mask structures. Scale bars are 500 µm.

on the precise quality evaluation of the sidewalls and dimension of the designs, optimized exposure parameters were administered in a single exposure step at 7 mW cm^{-2} for 6 min, as can be seen in Figure 1b. Based on the mask aligner system used in this work, the maximum allowed light intensity was 7 mW cm^{-2}. However, it can be predicted that using higher UV lamp energy, for instance, 500 W Hg, can result in decreasing the dimension and edge offsets of the features of the shadow mask.

To prove the effectiveness of the proposed technique in fabrication of the flexible shadow masks and characterize the properties of the fabricated shadow masks, the SU-8 shadow masks with various structure shapes, dimensions, and spacings were fabricated, as illustrated in Figure 1c. The images clearly demonstrate the high pattern flexibility of this shadow mask technology. The smallest feature size of around ≈10 µm was achieved using a 200 µm thick SU-8 shadow mask. However, by using thinner shadow masks, we can further decrease the dimension of the structures. The ability of the technique to engineer micropatterns with clean, smooth, and straight sidewalls was precisely evaluated by scanning electron microscope (SEM) studies. Moreover, fabrication of the thick shadow masks (≈500 µm) consisting of the structures with the length scale in the millimeter ranges (>3 mm) and only a few tens of micrometers in width (<40 µm) discovered the capability of the

process in providing high aspect ratio (>17:1) shadow mask structures.

One of the most important parameters of the stencil lithography is reusability of the shadow masks, which means the shadow masks can be reused many times, allowing a cost-effective pattern replication with various materials onto different substrates. One crucial factor, which can guarantee high reusability of the shadow masks, is the membrane stability. Although fabrication of the sub-micrometer apertures requires a significant reduction in thickness of the membrane, but normally this approach limits the stencil lithography to the single use because the membrane can be easily torn apart upon peeling off process. Thus, fabrication of the shadow masks with large enough thickness is required for high reusability degree as well as large-scale patterning process. In order to evaluate reusability of the fabricated shadow using our proposed method, we utilized a single SU-8 shadow mask with the thickness of 200 µm in 40 times deposition steps. In each deposition step, the SU-8 membrane was placed over a Si substrate and after evaporation of 50 nm Au was carefully peeled off from the substrate and reused without any deformation or any critical mechanical damages. Due to relatively large dimension of the features (>30 µm) compared to amount of the deposited materials, the mask holes did not get clogged up and the micropatterning process

**ADVANCED
SCIENCE NEWS**

www.advancedsciencenews.com

**ADVANCED
MATERIALS
TECHNOLOGIES**

www.advmattechnol.de

was effectively done in a reproducible manner. However, based on the precise SEM studies, we found a little degradation in quality of the sidewall of the shadow mask structures after multiple usages. The SEM images in **Figure 2**a illustrate the microstructures of a SU-8 shadow mask before usage and after 40 times deposition steps. As it can be clearly seen, due to accumulation of the deposited layers after 40 times usage, the angle of the microstructure sidewall has been slightly changed from the value of $\alpha_0 \geq 90°$ to the value around $\alpha_{40} \approx 80°$. It is worth to mention, accumulation of the deposited materials on the membrane and inside the apertures after many times usage can ultimately produce a significant reduction in the apertures size. In this case, a simple approach for reusing the masks is a cleaning process to selectively remove the accumulated materials.

In order to transfer a pattern to SU-8 layer, it is generally exposed using a mask aligner system, which consists of a UV light source and a photomask. The most employed photomasks are chromium masks consist in chromium opaque pattern areas deposited in high quality quartz plate with a very high transparency to UV radiation. Although these masks have high resolution and stability, but their fabrication process is very expensive. Here, we developed a fast and cost-effective process to fabricate a plastic photomask to simply pattern any desired microfeatures on SU-8 layer. The main requirements to be considered for selection of a plastic for the photomask are high transparency to UV light, high thermal and chemical stabilities. For this reason, cyclic olefin copolymer, which is known for its excellent optical properties, high glass-transition temperature, low shrinkage, and low moisture absorption was selected. By applying this self-made flexible plastic photomask, we successfully fabricated SU-8 shadow mask consisting of the microstructures with sharp edges (fabrication process of the plastic photomask is provided in the Experimental Section).

We employed both commercial chromium and self-made plastic photomasks for the fabrication of the SU-8 shadow masks to compare the edge quality of the shadow mask microstructures. Although, patterning by a commercial chromium photomask (80 nm Cr layer patterned on quartz plate) was done in hard contact mode, there was still a gap between the photomask and SU-8 layer because of the nonuniformity of the thick spin-coated SU-8 layer especially at the edges of the substrate. Presence of this air gap results in loss of the resolution and yield of the SU-8 structures with no-sharp edges.[45] As displayed in Figure 2b, by applying chromium photomask, the edge offset value as an indicator of the edge roughness of the shadow mask structures was measured around ≈15 µm. In comparison, the flexibility of the self-made plastic photomask enables us to directly lay it on the middle of the SU-8 layer, which is more uniform compared to the edges. This reduces the air gap between the photomask and SU-8 layer, and thereof
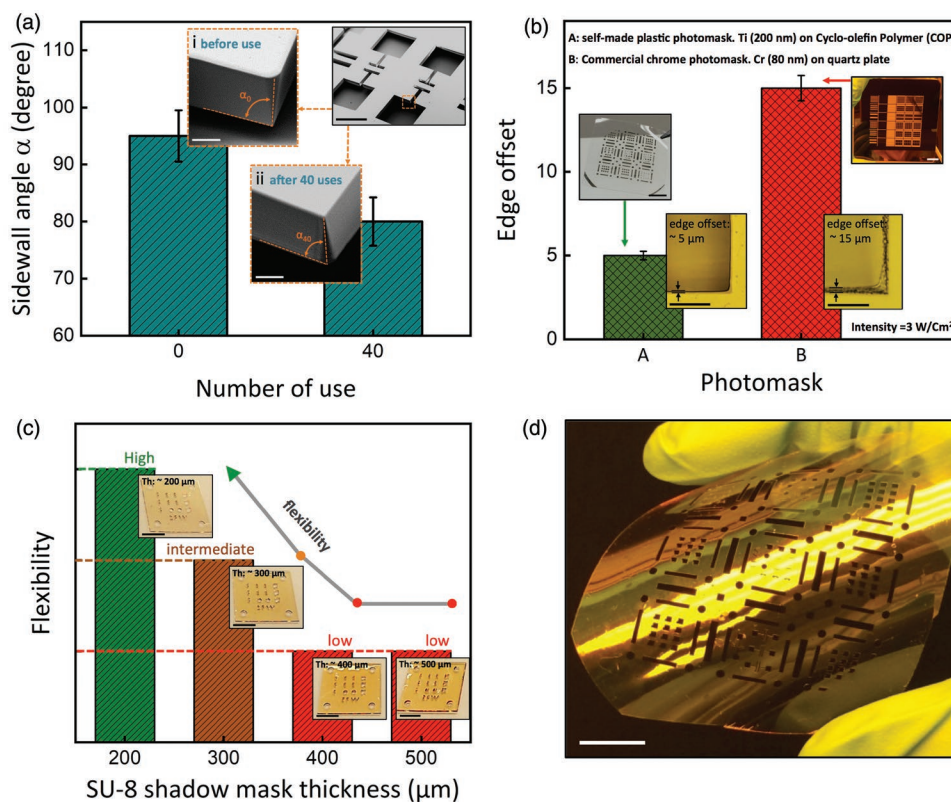

Figure 2. Characterization of the fabricated SU-8 shadow masks. a) Dependency of the sidewall angle of the shadow mask structures (α) to the number of use. The angle of α_0 is the sidewall angle of the shadow mask structures before use and α_{40} is the structure sidewall angle after 40 times deposition steps. Scale bar in the right inset SEM image is 1 mm and in the close-up SEM views are 50 µm. b) Comparison of the edge quality of the shadow mask structures fabricated by the self-made plastic photomask and the commercial chromium photomask. Scale bars in the optical photographs of the photomasks are 20 mm and in the magnified optical images of the structures corners are 100 µm. c) Displaying the dependency of the shadow mask flexibility to the shadow mask thickness. Scale bars are 5 mm. d) Photograph of a highly flexible 200 µm thick SU-8 shadow mask. Scale bar is 20 mm.

1900519 (4 of 9)

decreasing the diffraction effect in the interface of air and SU-8 layer during the exposure process. Employing the plastic photomask decreased the edge offset value to ≈5 µm and led to smooth and straight sidewalls in the shadow mask features.

By combining both spin-coating and volume-injection coating processes, we demonstrated the ability of the method to fabricate the uniform SU-8 films with various thicknesses. Surface tension and high mobility make SU-8 self-planarized and cause formation of the films with good flatness and uniformity during the soft baking process. We measured the thickness of a 200 µm thick SU-8 layer over a surface area of 14×14 mm^2 at different points. The thickness variation based on 20 measured points was calculated around 6%. The roughness measurement which was done by atomic force microscopy (AFM) revealed a root mean square roughness value of 0.26 nm for SU-8 layer with 200 µm thickness. The optical images in Figure 2c illustrate SU-8 shadow masks with different thicknesses ranging from 200 to 500 µm. The flexibility degree of the shadow masks can be tuned by varying the thickness of the shadow masks. As displayed in Figure 2c, by decreasing the thickness of the SU-8 layer from 500 to 200 µm, the amount of flexibility of SU-8 shadow masks remarkably increased. We found that the 200 µm thick shadow masks are highly flexible compared to the shadow masks with the thickness above 400 µm. Figure 2d displays a flexible 4 in. wafer size SU-8 shadow mask with the thickness of 200 µm, which can be utilized for large-scale micropatterning process on flexible substrates.

Stencil lithography is mostly limited to the single step patterning applications. However, multilayer surface patterning technology has numerous benefits such as fabricating fully functional devices by adding structured films layer by layer without the need for the multiple photolithography steps. But, in the multilayer patterning process using shadow masks, there are difficulties in aligning between the patterned layers. These difficulties can be addressed by using the built-in mechanical alignment structures. Different alignment features including the etched pyramids, v-grooves, jig, or high aspect ratio pillar structures have been reported for the multilayer micropatterning by means of shadow masks.[13,29,41,46] However, the applied fabrication methods often require complicated dry and wet chemical etchings and the aligning processes have to be done under microscopic tools. Here, high aspect ratio SU-8 pillars as alignment structures were designed to fix the shadow masks in place and align them with together. Unlike most of the widely used alignment techniques, the alignment process in this work can be done without using any microscopic tools, which can significantly simplify the alignment process and make it much faster. To create the alignment pillars, the same fabrication process for the SU-8 shadow masks was applied. **Figure 3**a shows the fabrication process of SU-8 pillars. First, a thick layer of SU-8 with the thickness around ≈700 µm is spin-coated on a Si substrate. Similar to the patterning process of the shadow masks, SU-8 pillars are structured using the self-made plastic photomask. After a long development process, followed by a hard baking step to further cross-link SU-8 layer, thick SU-8 pillars as alignment structures are formed on the substrate. The sequence of the alignment process using the vertical SU-8 pillars is displayed in Figure 3b. As it has been clearly shown, the fabricated SU-8 shadow masks with the hole

structures complementary to the pillars can be easily aligned into the alignment pillars by means of a tweezer and without using any optical microscope. As SU-8 pillars on the substrate can be tightly fixed into the holes of the shadow masks, no alignment failures can happen even if the substrate is completely faced down. However, the aligned shadow masks are mechanically robust enough to be easily released from the substrate after the deposition processes without any mechanical damage and can be further used.

To realize a multilayer micropatterning process by means of the fabricated SU-8 shadow masks and the alignment technique based on SU-8 pillars, two subsequent deposition steps through electron beam evaporation technique were carried out. The sequence of the multilayer surface patterning process with the mechanically aligned SU-8 shadow masks has been schematically illustrated in Figure 3c. The process begins with precisely aligning the first shadow mask into SU-8 pillars fabricated on the substrate surface. Then, a metal layer such as Au, Ti, or Cr is deposited onto the substrate. After removing the first shadow mask from the substrate without any sensible damage, the second SU-8 shadow mask is carefully placed inside the alignment structures. After the second deposition step and releasing the second shadow mask, the final pattern with two aligned metal layers can be achieved. To analyze the precision of the mechanical alignment technique, we evaporated two metallic layers including 20 nm Cr and 20 nm Au through two SU-8 shadow masks with complementary "E- shaped" patterns, as shown in Figure 3d. The E-shaped structure was used for the deposition of Cr layer and Au layer was patterned by the mirrored E-shaped (Ǝ) structures. Based on SEM studies, an x-offset of around ≈2 µm was achieved in the case patterning two E-shaped structures on top of each other. Larger x-offset value around ≈10 µm was measured when an E-shaped structure was patterned in front of a mirrored E-shaped feature. Moreover, y-offset of around ≈2 µm for both the cases was achieved. It is worth mentioning due to the blurring effect during the deposition of Au layer, slightly larger dimensions for the mirrored E-shaped structure was detected.

In order to evaluate the potential of our SU-8 shadow mask technology for pattering on the surfaces which are not well compatible with resist spinning and the associated chemical or thermal process steps, we applied our shadow mask methodology to realize the conductivity of a planar sheet of poly(3,4-ethylenedioxythiophene):polystyrene sulfonate (PEDOT:PSS). **Figure 4**a displays a pair of Au electrodes that have been patterned on this polymeric thin film through SU-8 shadow mask. The results of the conduction measurement on a patterned channel with the width of 200 µm and the length of 36 µm have been illustrated in Figure 4b. By applying a bias from −1.0 to 1.0 V between the two Au electrodes, the electric conduction demonstrates a perfect linear relationship with voltage. The conductivity of PEDOT was calculated as 990 S cm^{-1}, which corresponds to the expected property of a highly conductive PEDOT:PSS thin film.

To prove the ability of the SU-8 shadow mask technique for the large-scale surface patterning process, we fabricated a robust wafer-scale SU-8 shadow mask. The 200 µm thick SU-8 layer coated on a 4 in. Si wafer was patterned by a wafer-scale plastic photomask. Figure 4c shows the wafer-scale SU-8 shadow mask
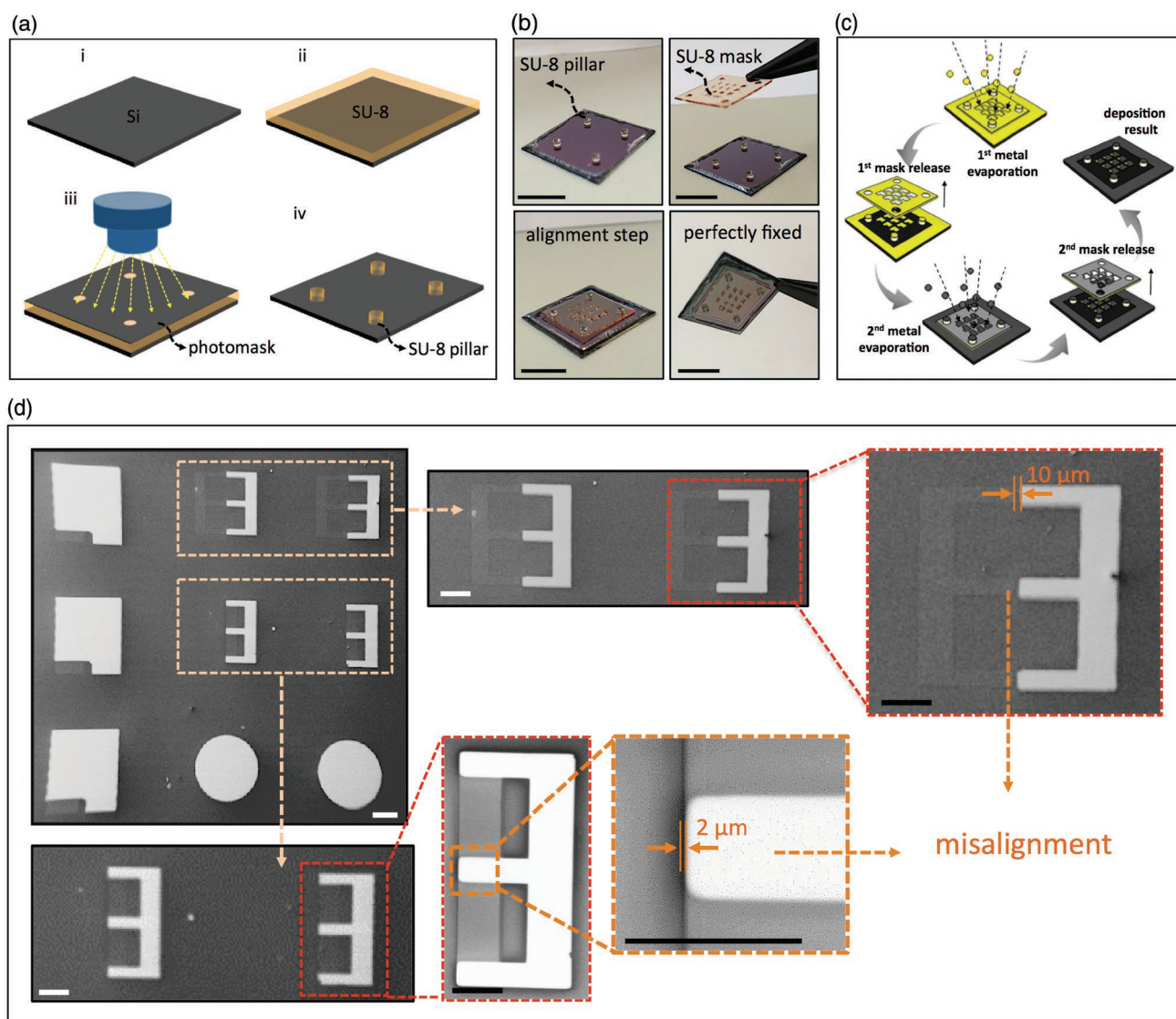
**ADVANCED
SCIENCE NEWS**
www.advancedsciencenews.com

**ADVANCED
MATERIALS
TECHNOLOGIES**
www.advmattechnol.de

Figure 3. Multilayer micropatterning process using SU-8 pillars as alignment structures. a) Fabrication process of the SU-8 pillars as the alignment structures. First, a thick layer of SU8 with the thickness around ≈700 µm is spin-coated on a Si substrate. SU-8 pillar is structured using a self-made plastic photomask. After a long development process, followed by a hard baking step, the thick SU-8 pillars as alignment structures are formed on the substrate. b) Sequence of the alignment process using the vertical SU-8 pillars. The fabricated SU-8 shadow mask with the predefined hole structures complementary to the pillars is easily aligned into the alignment structures by means of a tweezer and without using any optical microscope. Scale bars are 1 mm. c) Schematics showing the sequence of the steps for the multilayer micropatterning process by means of the SU-8 shadow masks and the proposed alignment technique. d) Evaluation of the alignment accuracy of the SU-8 pillars' alignment technique. Two metal layers of Cr with E-shaped patterns and Au with mirrored E-shaped structures were subsequently deposited to measure the alignment precision of the applied alignment technique. Scale bars are 200 µm.

and plastic photomask. Large-scale micropatterning process was done by using the fabricated wafer-scale SU-8 shadow mask and evaporation of 30 nm Cr layer on a 4 in. silicon wafer with predefined SU-8 alignment pillars, as shown in Figure 4d. High mechanical stability and flexibility degree of the large shadow mask enabled us to easily place it into the alignment structures on the wafer surface without any mechanical damage. The corresponding patterning result on the Si wafer is displayed in Figure 4e. The alignment accuracy of the transferred multiple patterns was measured by subsequent deposition of two metal layers of Au (30 nm) and Cr (30 nm). Based on the alignment precision measurements, the misalignment between the

wafer-scale shadow masks is between 9 and 15 µm, as displayed in Figure 4f.

In conclusion, we have developed a flexible, mechanically robust, and reusable shadow mask based on SU-8 polymer. This shadow mask technology has high pattern flexibility as various shapes with different dimensions can be created. Characterization of the fabricated shadow masks in terms of the resolution, reusability, and flexibility reveals the high potential of the proposed shadow mask technique for the simple micropatterning process at any surfaces that are not compatible with photolithographic patterning process. To render a multilayer micropatterning process by means of our shadow mask
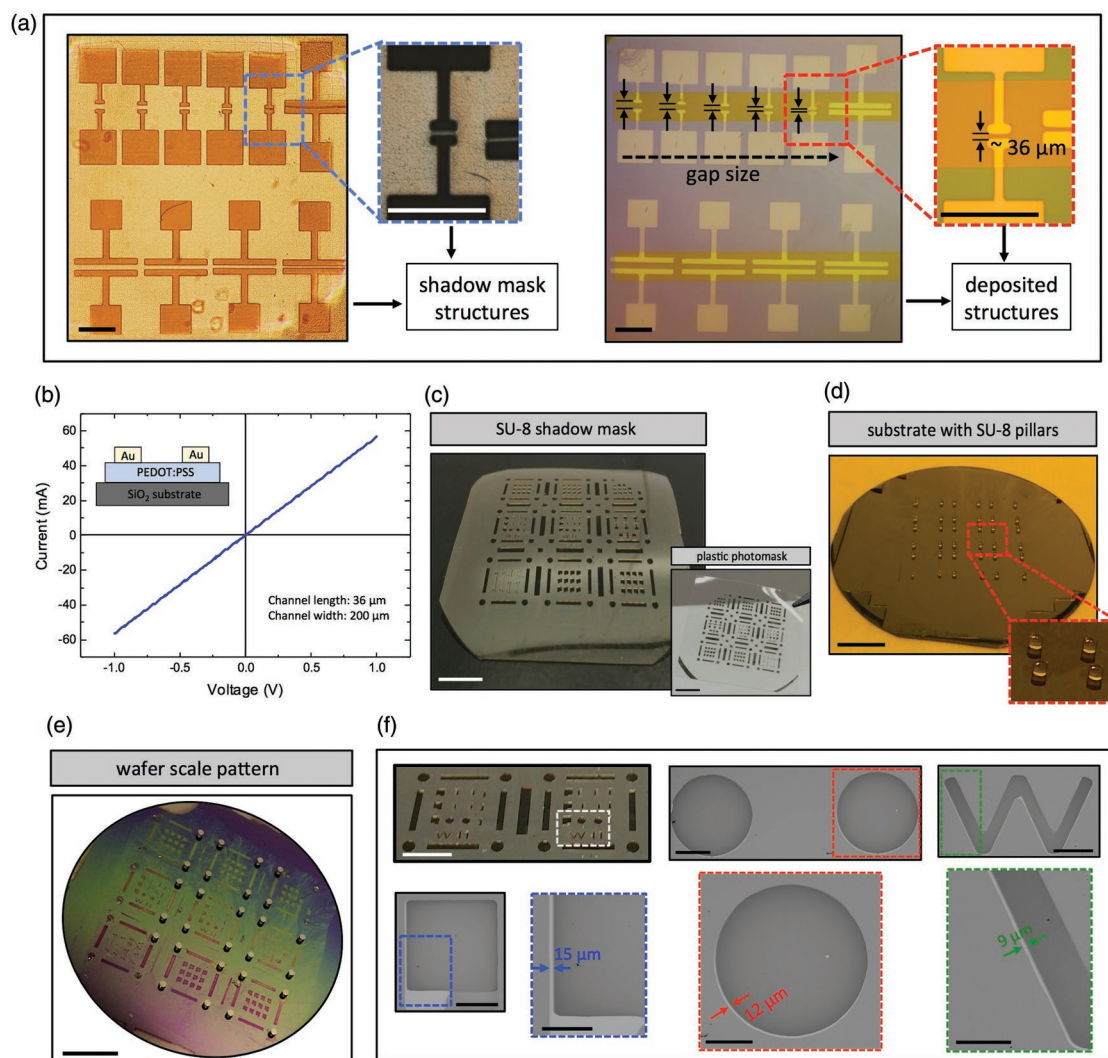
**ADVANCED
SCIENCE NEWS**
www.advancedsciencenews.com

**ADVANCED
MATERIALS
TECHNOLOGIES**
www.advmattechnol.de

Figure 4. SU-8 shadow mask applications. a) Micropatterning process on the organic thin films. Photographs showing patterning process of the electrodes on highly conductive organic PEDOT:PSS thin film using SU-8 shadow mask. Fabricated shadow mask provides the channel patterns with different width and length. Scale bars represent 1 mm. Scale bars in close-up images are 500 µm. b) Conductivity measurement of the PEDOT:PSS thin film using a channel with 200 µm width and 36 µm length. c) Optical image displays a wafer-scale SU-8 shadow mask fabricated by a wafer-scale plastic photomask. d) A 4 in. Si wafer with SU-8 pillars as the alignment structures. e) Wafer-scale micropatterning process is proved by evaporation of 30 nm Cr through the fabricated wafer size shadow mask, which is aligned into the SU-8 pillars on the Si wafer surface. Scale bars in (c)–(e) are 20 mm. f) Evaluation of the alignment accuracy of the transferred multiple patterns in the wafer-scale shadow mask for different structures by subsequent deposition of two metal layers of Au (30 nm) and Cr (30 nm). Scale bar in the shadow mask image is 10 mm. Scale bars in multiple patterns images and close-up images are 500 and 200 µm, respectively.

technology, we propose a simple and fast alignment technique based on the SU-8 pillars. SU-8 shadow masks with predefined holes can be easily aligned into the alignment pillars without using any optical microscope. Alignment accuracy of around ≈2 µm can be achieved using this alignment technique. High mechanical robustness and flexibility degree of the fabricated shadow mask make it compatible with wafer-scale micropatterning processes. We demonstrate an efficient large-scale multilayer micropatterning process by realization of highly reusable and flexible wafer-scale shadow masks and high-aspect ratio SU-8 pillars as alignment structures on a wafer-scale substrate. The ability of the process to provide ultrahigh aspect ratio (>17:1) shadow mask structures is also shown. Moreover,

capability of the proposed SU-8 shadow masks for micropatterning on organic thin films has been demonstrated by fabrication of the metallic contacts on a PEDOT sheet for the conductivity measurements without using any lithography and chemical processes.

Experimental Section

Preparation of the Adhesive PDMS Layer: PDMS (Sylgard 184 Silicone Elastomer, Dow Corning Corp.) was used as an adhesive layer prior to deposition of SU-8 layer. The preparation of PDMS solution involved mixing of the base and curing agent in a weight

ratio of 10:1, vigorous whisking of the mixture to make sure the curing agent was uniformly distributed, and finally keeping the mixture for 2 h in a dedicator to enable the trapped air bubbles to escape. Afterward, PDMS solution was spin-coated on a Si substrate at 1500 rpm for 45 s and followed by an annealing process at 120 °C for 20 min. Further, a 50 µm thick PI (DuPont Corporation) layer was adhered to the PDMS layer to be used as a releasing layer at the end of the fabrication process.

Preparation of SU-8 Layer: A new series of SU-8 photoresist (SU-8 3005, MicroChem Corp.) was spin-coated on top of the PI releasing layer in two separate steps. First, using a transfer pipet, a certain amount of SU-8 (0.5 mL) was introduced onto the PI layer and spin-coated at 500 rpm for 8 s. The second coating step was done at 300 rpm for 15 s, resulting in a layer thickness of 100 µm. To increase the thickness of SU-8 layer, the additional amounts of SU-8 should be added. The layers with the thicknesses of 200, 300, 400, and 500 µm were obtained by additional amounts of 0.1, 0.2, 0.3, and 0.4 mL to SU-8 layer, respectively.

SU-8 Patterning Process: After preparation of SU-8 layer, a prebaking process to evaporate the extra solvents and densify SU-8 layer was done on a typical hot plate in several steps. First, the substrate was baked at 65 °C for 10 min, then the temperature was ramped up to 95 °C and kept for 20 min. Afterward, the baking temperature was increased gradually to 120 °C. The duration of the final baking step was dependent on the thickness of SU-8 layer and was set to 60, 90, 120, and 150 min for SU-8 layer with the thicknesses of 200, 300, 400, and 500 µm, respectively. Further, the substrate was cooled down to 55 °C and kept for 15 min for the recrystallization process. Finally, the substrate was stored at room temperature for 15 min to be relaxed prior to UV exposure. The exposure process was done by a MJB4 mask aligner system (SUSS MicroTec) equipped with a 300 W Hg lamp, which could provide the maximum light intensity of 7 mW cm^{-2}. Similar to the prebaking process, the postbaking was done in several steps. First, the temperature was gradually increased from the room temperature to 65 °C and kept for 15 min at this temperature. In the second step, depending on the final SU-8 layer thickness, the sample was baked at 95 °C for different durations. The optimal baking time was 30 min for the layer thicknesses of 200 and 300 µm and 40 min for the thicknesses of 400 and 500 µm. Development process was done in propylene-glycol-methyl-ether-acetate (PGMEA) developer (MicroChem Corp.) in an ultrasonic bath and followed by immersing in isopropyl alcohol (IPA). Depending on the thickness of SU-8 layer, the developing process lasted between 20 and 30 min.

Preparation of the Plastic Photomask: To prepare the plastic photomask, ZeonorFilm ZF 16 (ZEON Corp.) with the thickness of 100 µm, transparency of 92%, and the glass temperature of 100 °C was used. For the patterning process, the plastic film was temporarily adhered to a Si substrate, which was covered by a PDMS layer. The image reversal photoresist of AZ5214E (MicroChem Corp.) was spin-coated on the plastic layer at 6000 rpm for 45 s and then was baked for 4 min on a hot plate at 90 °C. The exposure process was done by µPG 501 maskless aligner machine (Heidelberg). After postbaking process for 2 min at 120 °C which was followed by 30 s flood exposure by SUSS MJB4 mask aligner machine (SUSS MicroTec), development process was carried out in AZ726 MIF (MicroChem Corp.) for 50 s. Afterward, 200 nm Ti was evaporated on the film and then lifted off.

Morphology Characterization of SU-8 Layers: Morphology investigation of SU-8 layers including thickness and surface roughness was done using Stylus Profilometer (Veeco Dektak-8) and AFM (Agilent 5600LS system) under an argon controlled environment.

Preparation of SU-8 Pillars: First, a thick layer of SU-8 was spin-coated on a Si substrate with dimension of 20×20 mm^2. The thick SU-8 layer was prepared in two steps. In the first step, 0.5 mL SU-8 was spin-coated in two cycles at 500 and 300 rpm for 8 and 15 s, respectively. Afterward, the sample was heated on a typical hot plate at 65 and 95 °C for 10 and 20 min, respectively. In the second step, an additional amount of 0.5 mL SU-8 was injected over the surface while the sample was on the hot plate at 95 °C. The temperature was slowly increased to 120 °C and the sample was baked at this temperature for 2 h. After cooling down, the thermal treatment process was repeated for 2 times more. This coating process resulted in a 700 µm thick SU-8 layer. The exposure process was done for 2 min through a fabricated plastic photomask using a SUSS MJB4 mask aligner system (SUSS MicroTec) equipped with a 300 W Hg lamp. Baking step was done at 65 and 95 °C for 15 and 50 min, respectively. Development was done in PGMEA developer (MicroChem Corp.) under ultrasonic condition for 30 min and followed by immersing in IPA. A hard baking step was followed at 120 °C for 1 h to further cross-link the SU-8 layer. Diameter of the circular structures on the photomask for patterning the pillars was designed 30 µm smaller than the hole diameter in the SU-8 shadow mask.

Organic Layer Preparation: To prepare the organic thin layer, PEDOT:PSS solution (Heraeus Co.) was spin-coated on a Si substrate at 3000 rpm for 30 s, resulting in a 100 nm thick layer.

Electrical Measurements: A probe station and Keithley 2636A were used to characterize the in-plane current–voltage properties of the organic thin layer by applying a bias from −1.0 to 1.0 V between the Au electrodes.

Conflict of Interest

The authors declare no conflict of interest.

[1] H. G. Craighead, *Science* **2000**, *290*, 1532.
[2] J. Brugger, J. W. Berenschot, S. Kuiper, W. Nijdam, B. Otter, M. Elwenspoek, *Microelectron. Eng.* **2000**, *53*, 403.
[3] E. Menard, M. A. Meitl, Y. Sun, J. Park, D. J. Shir, Y. Nam, S. Jeon, J. A. Rogers, *Chem. Rev.* **2007**, *107*, 1117.
[4] O. Vazquez-Mena, L. Gross, S. Xie, L. G. Villanueva, J. Brugger, *Microelectron. Eng.* **2015**, *132*, 236.
[5] K. Sidler, N. V. Cvetkovic, V. Savu, D. Tsamados, A. M. Ionescu, J. Brugger, *Procedia Chem.* **2009**, *1*, 762.
[6] O. Vazquez-Mena, T. Sannomiya, M. Tosun, L. G. Villanueva, V. Savu, J. Voros, J. Brugger, *ACS Nano* **2012**, *6*, 5474.
[7] D. Sacchetto, S. Xie, V. Savu, M. Zervas, G. De Micheli, J. Brugger, Y. Leblebici, *Microelectron. Eng.* **2012**, *98*, 355.
[8] D. Sacchetto, V. Savu, G. De Micheli, J. Brugger, Y. Leblebici, *Microelectron. Eng.* **2011**, *88*, 2732.
[9] M. Aljada, K. Mutkins, G. Vamvounis, P. Burn, P. Meredith, *J. Micromech. Microeng.* **2010**, *20*, 1.
[10] Y. X. Zhou, A. T. Johnson, J. Hone, W. F. Smith, *Nano Lett.* **2003**, *3*, 1371.

1900519 (8 of 9)

[11] S. Aksu, A. A. Yanik, R. Adato, A. Artar, M. Huang, H. Altug, *Nano Lett.* **2010**, *10*, 2511.

[12] J. Wu, M. Zhang, L. Chen, V. Yu, J. T. Wong, X. Zhang, *RSC Adv.* **2011**, *1*, 746.

[13] A. Tixier, Y. Mita, J. P. Gouy, H. Fujita, *J. Micromech. Microeng.* **2000**, *10*, 157.

[14] P. B. Agarwal, S. Pawar, S. M. Reddy, P. Mishra, A. Agarwal, *Sens. Actuators, A* **2016**, *242*, 67.

[15] S. Xie, V. Savu, W. Tang, O. Vazquez-mena, K. Sidler, H. Zhang, *Microelectron. Eng.* **2011**, *88*, 2790.

[16] H. Tao, L. R. Chieffo, M. A. Brenckle, S. M. Siebert, M. Liu, A. C. Strikwerda, K. Fan, D. L. Kaplan, X. Zhang, R. D. Averitt, *Adv. Mater.* **2011**, *23*, 3197.

[17] K. Sidler, L. G. Villanueva, O. Vazquez-Mena, V. Savu, J. Brugger, *Nanoscale* **2012**, *4*, 773.

[18] S. Azimi, J. Song, C. J. Li, S. Mathew, M. B. H. Breese, T. Venkatesan, *Nanotechnology* **2014**, *25*, 445301.

[19] S. Ghadarghadr, C. P. Fucetola, L. L Cheong, E E Moon, H. I. Smith, *J. Vac. Sci. Technol., B: Microelectron. Nanometer Struct.–Process., Meas., Phenom.* **2011**, *29*, 06F401.

[20] W. J. Hyun, E. B. Secor, M. C. Hersam, C. D. Frisbie, L. F. Francis, *Adv. Mater.* **2015**, *27*, 109.

[21] S. M. Yi, S. H. Jin, J. D. Lee, C. N. Chu, *J. Micromech. Microeng.* **2005**, *15*, 263.

[22] Y. Yao, Y. Jia, F. Chen, S. Akhmadaliev, S. Zhou, *Appl. Opt.* **2014**, *53*, 195.

[23] I. Chung, J. Kim, K. Kang, *Int. J. Precis. Eng. Manuf.* **2009**, *10*, 11.

[24] J. Heo, H. Min, M. Lee, *Int. J. Precis. Eng. Manuf.* **2015**, *2*, 225.

[25] M. R. H. Knowles, G. Rutterford, D. Karnakis, A. Ferguson, *Int. J. Adv. Manuf. Technol.* **2007**, *33*, 95.

[26] K. Du, J. Ding, Y. Liu, I. Wathuthanthri, C. Choi, *Micromachines* **2017**, *8*, 131.

[27] P. Jothimuthu, A. Carroll, A. Asgar, S. Bhagat, G. Lin, J. E. Mark, I. Papautsky, *J. Micromech. Microeng.* **2009**, *19*, 045024.

[28] A. Folch, B. Jo, O. Hurtado, D. J. Beebe, M. Toner, *J. Biomed. Mater. Res.* **2000**, *52*, 346.

[29] S. Selvarasah, S. H. Chao, C. Chen, S. Sridhar, A. Busnaina, A. Khademhosseini, M. R. Dokmeci, *Sens. Actuators, A* **2008**, *145–146*, 306.

[30] S. Ravi-Kumar, B. Lies, X. Zhang, H. Lyu, H. Qin, *Polym. Int.* **2019**, *68*, 1391.

[31] S. Hwang, X. Huang, J. Seo, J. Song, S. Kim, S. Hage-Ali, H. Chung, H. Tao, F. G. Omenetto, Z. Ma, J. Rogers, *Adv. Mater.* **2013**, *25*, 3526.

[32] K. Yong, A. Ashraf, P. Kang, S. Nam, *Sci. Rep.* **2016**, *6*, 24890.

[33] Y. Kajiyama, K. Joseph, K. Kajiyama, S. Kudo, H. Aziz, *Appl. Phys. Lett.* **2014**, *104*, 053303.

[34] S. Rahiminejad, E. Köhler, P. Enoksson, *J. Phys.: Conf. Ser.* **2016**, *757*, 012021.

[35] N. Sowmya, N. Oraon, S. Sen, M. Rao, *IEEE International Conference on Electronics*, Computing and Communication Technologies (CONECCT), Bangalore **2015**.

[36] D. M. Ornoff, Y. Wang, N. L. Allbritton, *J. Micromech. Microeng.* **2012**, *23*, 025009.

[37] K. Du, Y. Liu, I. Wathuthanthri, C. H. Choi, *J. Vac. Sci. Technol., B: Nanotechnol. Microelectron.: Mater., Process., Meas., Phenom.* **2013**, *31*, 06FF04.

[38] K. Du, Y. Liu, I. Wathuthanthri, C. H. Choi. *J. Vac. Sci. Technol., B: Nanotechnol. Microelectron.: Mater., Process., Meas., Phenom.* **2012**, *30*, 06FF04.

[39] J. Y. Park, D. H. Lee, E. J. Lee, S. Lee, *Lab Chip* **2009**, *9*, 2043.

[40] M. Graff, S. K. Mohanty, E. Moss, A. B. Frazier, *J. Microelectromech. Syst.* **2004**, *13*, 956.

[41] G. Kim, B. Kim, J. Brugger, *Sens. Actuators, A* **2003**, *107*, 132.

[42] J. Choi, A. Roychowdhury, N. Kim, D. E. Nikitopoulos, W. Lee, H. Han, S. Park, *J. Micromech. Microeng.* **2010**, *20*, 085011.

[43] M. Agirregabiria, F. J. Blanco, J. Berganzo, M. T. Arroyo, A. Fullaondo, K. Mayora, J. M. Ruano-López, *Lab Chip* **2005**, *5*, 545.

[44] C. Lin, G. Lee, B. Chang, G. Chang, *J. Micromech. Microeng* **2002**, *12*, 590.

[45] J. Zhang, M. B. Chan-park, S. R. Conner, *Lab Chip* **2004**, *4*, 646.

[46] J. Brugger, C. Andreoli, M. Despont, U. Drechsler, H. Rothuizen, P. Vettiger, *Sens. Actuators, A* **1999**, *76*, 329.